Role of Fluorodeoxyglucose Positron Emission Tomography/Computed Tomography in Various Orbital Malignancies

Abstract

Orbital swelling comprises wide spectrum of pseudotumors, benign and malignant tumor. Malignant tumor may be primary or secondary tumor, and they constitute about 36% of orbital tumors in adult. Fluorodeoxyglucose-positron emission tomography/computed tomography (FDG-PET/CT) scan is extensively used in hematological malignancies and in solid tumors for staging, treatment response, and restaging. Recently, the use of FDG-PET/CT in orbital malignancies has gained importance. The aim of this pictorial essay is to illustrate few important orbital malignancies detected in F-18 FDG-PET/CT and discuss its role in assessing the primary lesion and associated systemic finding.

Keywords: *Fluorodeoxyglucose, malignancy, orbital, positron emission tomography/computed tomography*

Aravintho Natarajan, Piyush Chandra, Nilendu Purandare, Archi Agrawal, Sneha Shah, Ameya Puranik, Venkatesh Rangarajan

Department of Nuclear Medicine, Tata Memorial Hospital, Mumbai, Maharashtra, India

Introduction

Orbital swelling comprises wide spectrum of pseudotumors, benign and malignant tumor. Malignancy constitutes about 36% of orbital tumors in adult and may be classified as primary orbital tumor or secondary deposit from primary elsewhere. Based on the location, it can be intraocular or extraocular tumor, where the extraocular tumors can be further classified into intraconal and extraconal [Table 1].[1] Computed tomography (CT) is the initial of choice of investigation for evaluating orbital tumors, especially for bony detail and calcifications, whereas magnetic resonance imaging (MRI) is superior for evaluation of the visual pathways, the globe, and soft tissues. Fluorodeoxyglucose-positron emission tomography/CT (FDG-PET/CT) is less often used in characterization of the primary orbital mass and is more useful in staging of the pathological proven primary orbital malignancies, assessing response to treatment and evaluation of disease recurrence.

In this pictorial review, we have illustrated few important orbital malignancies detected in FDG-PET/CT and discussed its role in assessing the primary lesion and the associated systemic findings.

Anatomy

The orbit is divided into the globe, extraocular muscles and intraconal and extraconal spaces. The muscle cone formed by all the extraocular muscles except the inferior oblique separates the intraconal and extraconal spaces [Figure 1]. The globe is continuous with the central nervous system and consists of three distinct layers, namely, the sclera, uvea, and retina. The bony orbit is a pyramidal structure formed by seven skull bones. Erosion of bony orbit usually suggests aggressive pathology. A dedicated CT of the orbit in the PET/CT protocol can be acquired using 0.6–1 mm thin slices after intravenous injection of iodinated contrast material for precise depiction of the globe, optic nerve, intraconal, and extraconal spaces with standard coronal and sagittal reconstructions. CT scan plays important role especially in evaluating calcification of the orbital tumor, bony erosion, and extension to adjacent sinonasal structure or intracranial extension.

Normal Appearance of Orbit on Fluorodeoxyglucose-positron Emission Tomography/Computed Tomography

Intense FDG uptake is noted symmetrically in bilateral extraocular muscles; optic nerve and rarely low-grade FDG uptake may be also noted in both the eyelid muscles [Figure 1]. Rest of the orbit does not show any significant FDG uptake. Any asymmetry in the FDG uptake or abnormal

This is an open access journal, and articles are distributed under the terms of the Creative Commons Attribution-NonCommercial-ShareAlike 4.0 License, which allows others to remix, tweak, and build upon the work non-commercially, as long as appropriate credit is given and the new creations are licensed under the identical terms.

For reprints contact: reprints@medknow.com

How to cite this article: Natarajan A, Chandra P, Purandare N, Agrawal A, Shah S, Puranik A, *et al.* Role of fluorodeoxyglucose positron emission tomography/computed tomography in various orbital malignancies. Indian J Nucl Med 2018;33:118-24.

Address for correspondence:
Dr. Venkatesh Rangarajan, Department of Nuclear Medicine, Tata Memorial Hospital, Mumbai, Maharashtra, India.
E-mail: drvrangarajan@gmail.com

Access this article online

Website: www.ijnm.in

DOI: 10.4103/ijnm.IJNM_135_17

Quick Response Code:

© 2018 Indian Journal of Nuclear Medicine | Published by Wolters Kluwer - Medknow

sites of increased FDG uptake in the orbit (such as lacrimal gland, choroid, posterior ocular bulb, and prosthesis) should prompt the reader to explore an underlying pathology. Asymmetry in the normal uptake of FDG-PET/CT in extraocular/eyelid muscles is very sensitive in identifying cranial nerve pathologies [Figure 2] (for example, perineural spread of head/neck malignancies and brain metastasis).[2]

Ocular Melanoma

Uveal melanomas are the most common primary intraocular tumors in adults. They rise predominantly from the choroid and less commonly from the iris and ciliary body. On CT, choroidal melanoma appears as hyperdense choroidal mass. Although metastases at initial presentation are rare, almost 50% of patients in the course of the disease develop distant metastases. The incidence of distant metastases increases with increasing tumor thickness >10 mm, increasing patient age, presence of subretinal fluid or hemorrhage, and loss of chromosome 3 on cytogenetic studies. Freton *et al*. evaluated the role of FDG-PET/CT in staging choroidal melanomas in 330 consecutive patients. PET/CT identified distant metastasis at presentation in about 20% patients with the American Joint Committee on Cancer T4 disease. The most common site of metastases was liver followed by bone [Figures 3 and 4]. In addition, synchronous nonocular second malignancies were noted in 3.3% of patients.[3] PET/CT appears to be more sensitive than liver enzyme assays for screening and detection of liver metastases.[4]

Nonuveal melanomas can arise from the conjunctiva or skin of the eyelids. Conjunctival melanomas comprise 5% of intraocular melanomas, showing a significant increasing incidence rates in the western population past few decades. Locoregional spread is usually seen to preauricular and submandibular nodes. Distant metastases are however rare, compared to the uveal melanomas and seen in up to 16% at 5 years. PET/CT was evaluated in

Table 1: Classification of orbital tumors based on location

Intraocular tumours	Extraocular tumors	
	Extraconal	Intraconal
Retinoblastoma	Ocular adnexal lymphoma*	Optic nerve glioma
Intraocular melanoma	Metastases*	Optic nerve meningioma
Intraocular metastases	Rhabdomyosarcoma*	
Intraocular lymphoma	Granulocytic sarcoma*	
	Extraocular melanoma*	
	Sebaceous gland carcinoma	
	Lacrimal sac carcinoma	
	Peripheral nerve sheath tumor of orbit	

*Can also present as intraconal mass but less frequently

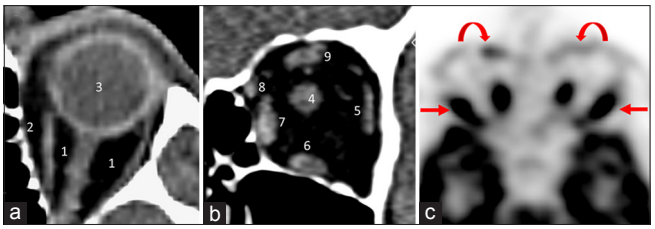

Figure 1: Anatomy of the orbit: Axial computed tomography image (a) shows the compartments of orbit, coronal computed tomography image (b) shows the extraocular muscles and axial fluorodeoxyglucose image (c) demonstrates the physiological pattern of symmetrical intense fluorodeoxyglucose uptake in bilateral extraocular muscles (arrow) and low-grade uptake in eyelids (curved arrow). (1. intraconal space, 2. extraconal space, 3. globe, 4. optic nerve, 5. lateral rectus, 6. inferior rectus, 7. medial rectus, 8. superior oblique, and 9. superior rectus)

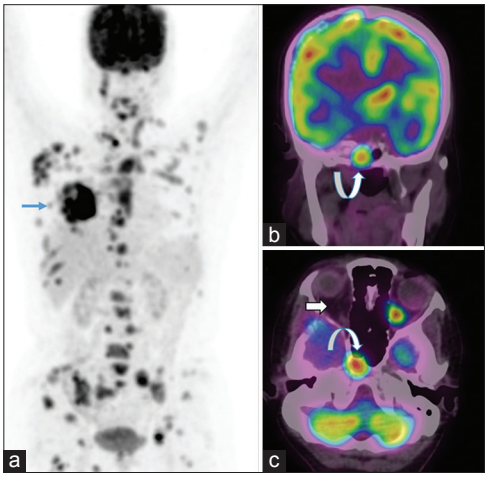

Figure 2: Asymmetrical fluorodeoxyglucose uptake in oculomotor nerve palsy: A 50-year-old female presented with right breast lump and double vision. Biopsy of breast mass confirmed diagnoses of infiltrating ductal carcinoma. Maximum intensity projection image (a) of fluorodeoxyglucose positron emission tomography/computed tomography shows uptake in right breast mass (arrow) and extensive skeletal metastases. Coronal (b) and axial (c) fusion images reveal lesion in right greater wing and body of sphenoid compressing (curved arrow) and causing palsy of oculomotor nerve, as demonstrated by the asymmetrical decreased fluorodeoxyglucose uptake in right extraocular muscles (block arrow)

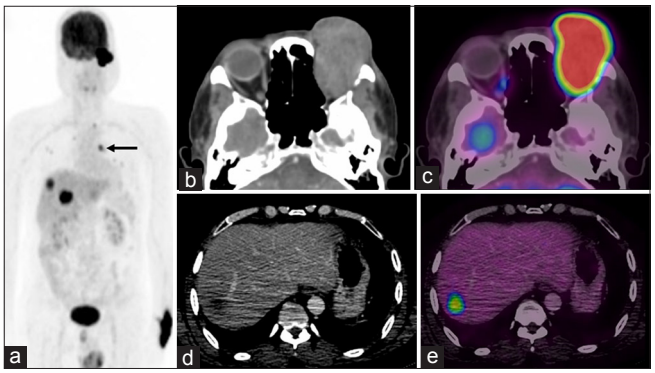

Figure 3: Primary orbital malignant melanoma: A 52-year-old patient who was diagnosed with orbital malignant melanoma following left exenteration, presented with recurrent swelling. Images of the fluorodeoxyglucose positron emission tomography/computed tomography scan (a) shows hypermetabolic recurrent left orbital mass (b and c) and metastases to lung (arrow) and liver (d and e)

staging 14 patients with T3–T4 conjunctival melanoma and did not reveal metastases in any, suggesting that PET/CT might not have a role in staging these subtypes of ocular melanomas.[5]

Sebaceous Gland Tumors

Sebaceous gland carcinomas (SGC) of eyelids are second most common tumor to involve the eyelid after basal cell carcinoma. These are rare slow-growing tumors, seen predominantly in elderly females. They arise from Meibomian glands, glands of Zeis, or glands associated with the caruncle. They often masquerade clinically as blepharoconjunctivitis or limbic keratoconjunctivitis and diagnosis of malignancy might be delayed. The common sites of the locoregional spread appear to be in orbit, submandibular, and intraparotid nodes [Figure 5]. Due to inadequate treatment at initial presentation, local recurrence is frequent and seen in up to 16%–30% patients. Distant metastases can be seen in 8%–40%, spreading commonly to lungs, pleura, and liver. Higher incidence of metastases are seen in patients with delay in diagnosis (duration of symptoms >6 months), patients with poorly differentiated tumors, size of eyelid tumors >10 mm, infiltration of blood vessels, multicentric origin, and pagetoid spread on histopathology.[6]

Role of FDG-PET/CT in diagnostic evaluation of SGC is very limited due to rarity of the disease. Baek *et al*. studied the role of PET/CT in 15 patients with periorbital malignancies which included 6 patients with sebaceous cell carcinoma. Diagnostic accuracy of PET/CT and CT for identification of nodal disease was 98% and 84% respectively. The tumors showed good FDG uptake.[7] Early and more accurate detection of nodal disease, early detection of recurrence, and identification of distant metastases at staging or restaging are potential indications of PET/CT in SGC that can impact treatment decision-making.

Lacrimal Sac Carcinoma

Primary carcinomas of lacrimal sac are rare malignancy with transitional carcinoma being the common histological subtype after squamous cell carcinoma. Owing to the hidden location within orbit, these tumors have insidious course and present in late stage with symptoms of dacryocystitis and nasolacrimal duct obstruction. Treatment includes wide local excision with adjuvant radiotherapy; however, transitional cell carcinoma has poor prognosis. Review of literature by Preechawai *et al*. described that one-third of patients have recurrent disease with a 22% rate of distant metastasis to the lungs. The overall mortality rate was 44%.[8] Thus, complete preoperative staging and early detection of disease recurrence is crucial for appropriate treatment to prolong the survival [Figure 6]. Owing to the rarity of the disease, only few case reports exist in literature demonstrating the utility of PET/CT in staging and surveillance of lacrimal sac carcinoma.[9]

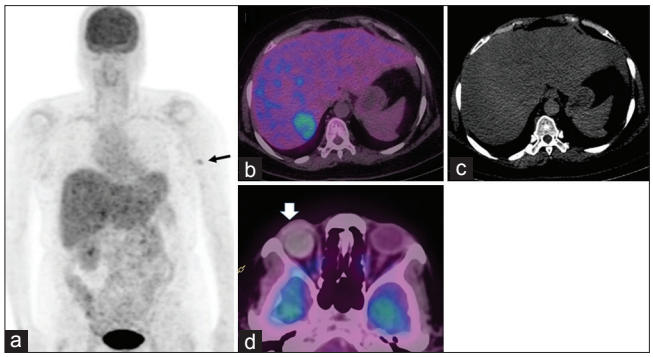

Figure 4: Recurrence of choroidal melanoma: Case of choroidal melanoma of the right eye, postenucleation was on routine follow-up. Maximum intensity projection image (a) of the fluorodeoxyglucose positron emission tomography/computed tomography scan shows focal uptake in marrow of the left humerus (arrow), further focal tracer uptake in posterior segment of liver was visualized in axial fusion image (b) and no obvious morphological change was noted in corresponding computed tomography image (c). Postenucleation status with ocular prosthesis (block arrow) was noted in the right orbit (d). Subsequently, fine-needle aspiration cytology of the liver lesion was done, which confirmed the diagnosis of metastatic malignant melanoma

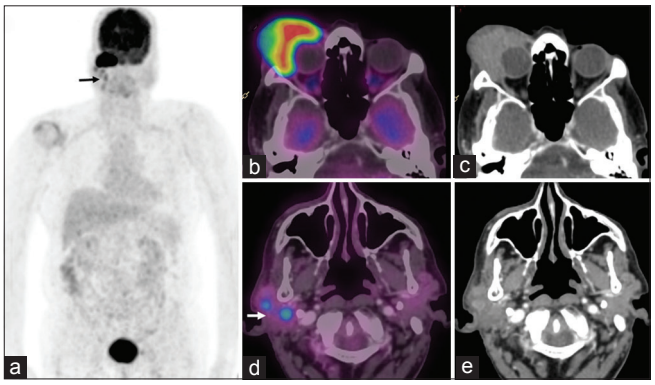

Figure 5: Sebaceous gland carcinoma: A 71-year-old male presented with swelling of right upper lid and fine-needle aspiration cytology of the swelling was suggestive of sebaceous cell carcinoma. Maximum intensity projection image (a) of the fluorodeoxyglucose positron emission tomography/computed tomography shows uptake in right orbital region and in right parotid region (arrow). Axial images (b and c) shows the right upper lid mass and metastatic right intraparotid nodes (d and e)

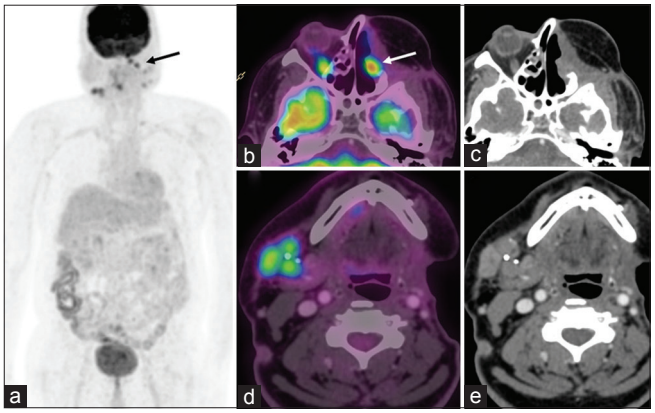

Figure 6: Recurrence of transitional cell carcinoma of lac sac: A 48-year-old male who is a treated case of transitional cell carcinoma left lacrimal sac was suspected for disease recurrence. Fluorodeoxyglucose positron emission tomography/computed tomography images (a-c) revealed recurrence in the flap (arrows) and metastatic right submandibular node (d and e)

Rhabdomyosarcoma of Orbit

It is most common soft-tissue sarcoma in the head neck in pediatric age group and comprises 10% of all malignancies of the orbit. On CT, it appears as ill-defined soft-tissue mass in extraconal space with erosion of the bony orbit in about 40%. Most lesions show aggressive local spread with extraorbital spread to sinonasal region and intracranial region. Of all the rhabdomyosarcoma (RMS), pediatric orbital RMS shows the most favorable outcome [Figure 7] to multimodality treatment with 5-year survival ranging from 80% to 90%. Embryonal RMS is most common histological subtype followed by pleomorphic and alveolar. Nodal metastasis is very uncommon in the orbital RMS due to scarce lymphatics in the posterior orbit. Nodal and distant metastases may be seen more frequently with aggressive histopathological features such as an alveolar subtype having a PAX3-FKHR fusion protein [Figure 8]. Multiple studies have successfully demonstrated the clinical utility of FDG-PET/CT in staging childhood RMS and predicting treatment outcomes. However, these were done in RMS predominantly arising from extremities and being of alveolar subtype. Currently, there is not enough evidence to suggest routine use of PET/CT in orbital RMS at present.[10,11]

Retinoblastoma

These are the most common malignant ocular tumors in children. Multimodality treatment has led to improved outcomes over last few decades; ultrasonography and CT are initial investigations of choice for tumor characterization. CT demonstrates the calcification in the intraocular mass, which has high sensitivity and specificity for the diagnosis of retinoblastoma [Figure 9]. MRI is the best imaging modality to assess optic nerve involvement and extraocular extension. Delay in diagnosis, extrascleral extension, optic nerve involvement, and bilateral disease are associated with higher incidence of metastatic disease.[12] FDG-PET/CT does not have a role in routine diagnostic evaluation of retinoblastoma, except in cases where distal metastasis is clinically suspected [Figure 9]. PET/CT can be also useful in treatment response evaluation of advanced tumors. Prognostic use of PET/CT in retinoblastoma was explored in a prospective study done by Radhakrishnan *et al*. where they showed that postneoadjuvant chemotherapy response based on the European Organization for the Research and Treatment of Cancer criteria is a strong predictor of event-free survival and overall survival (OS) in Stage III International Neuroblastoma Staging System retinoblastoma.[13]

Lymphoma

Orbital lymphoma is relatively rare condition constituting of about 8%–10% of extranodal Non-Hodgkin's lymphoma (NHL).[14] Based on the site of involvement, it is classified as ocular adnexal (OAL) and intraocular lymphoma. Primary intraocular lymphoma is extremely rare and is a subset of primary central nervous system lymphoma. Although OAL is also uncommon, it is the most common orbital malignancy in adults.[1] OAL is mostly extraconal in location and frequently occurs in superolateral quadrant of orbit and typically molds to the adjacent orbital structures. Bone erosion is uncommon. OAL is invariably NHL and mucosa-associated lymphoid tissue [Figure 10] being the most common subtype followed by diffuse large cell lymphoma (DLBCL). Systemic manifestation is noted in about 20% of the cases at presentation and 30% of cases with only orbital disease relapse with systemic lymphoma during follow-up.[15] Radiotherapy is the mainstay of treatment of disease confined to orbit, and chemotherapy is offered in case of high-grade NHL (DLBCL) [Figure 11] and in patients with systemic disease. Since most orbital lymphoma are low-grade lymphoma and show variable FDG avidity, the role of PET has not been clear in the past. However, evidences are mounting in favor of the

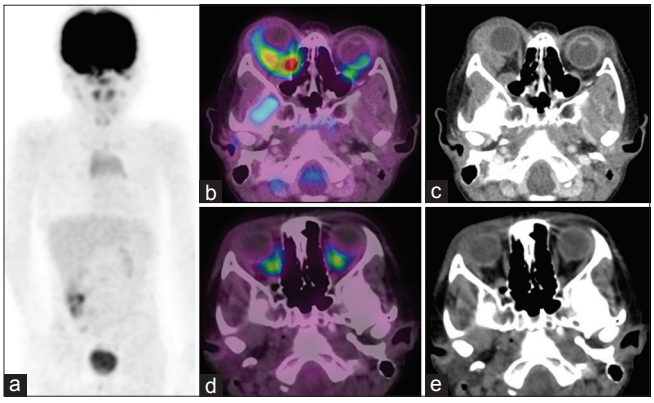

Figure 7: Treatment response of orbital rhabdomyosarcoma: A 10-year-old boy with right orbital swelling was diagnosed with embryonal rhabdomyosarcoma. Baseline fluorodeoxyglucose positron emission tomography/computed tomography scan images (a-c) show hypermetabolic right orbital mass and no evidence of distant metastases. Complete metabolic response of the orbital mass was noted in the posttherapy scan image (d-e) following chemotherapy and radiotherapy

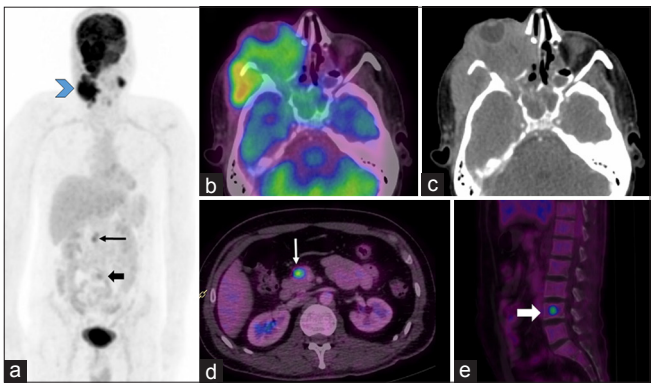

Figure 8: Alveolar rhabdomyosarcoma: fluorodeoxyglucose positron emission tomography/computed tomography images of a case of adult orbital alveolar rhabdomyosarcoma show hypermetabolic soft-tissue mass in right orbit with extraorbital extension (b and c) and metastatic cervical nodes (arrowhead). Focal uptake noted in the abdomen (arrow) and pelvic region (block arrow) in the maximum intensity projection (a) corresponds to pancreatic (d) and skeletal metastases (e)

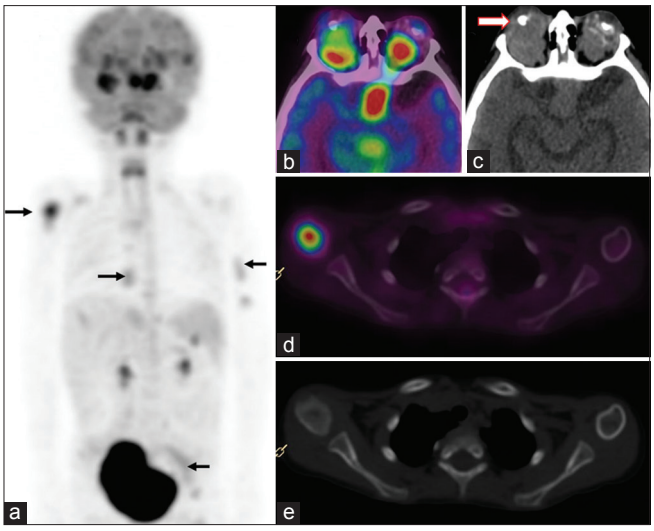

Figure 9: Bilateral retinoblastoma: A 7-year-old boy presented with bilateral orbital swelling and was diagnosed with bilateral retinoblastoma. Maximum intensity projection image (a) of the fluorodeoxyglucose positron emission tomography/computed tomography scan shows focal uptake in multiple sites in skeletal system (arrow) apart from the uptake in both the orbital region. Note the calcification (block arrow) of the ocular masses in the axial images (b and c) which is characteristic of retinoblastoma. Coronal fusion (d) and computed tomography image (e) shows metastases to right humerus

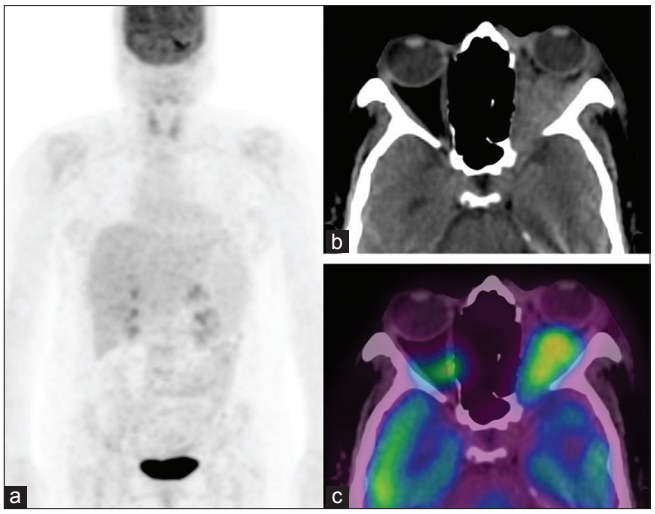

Figure 10: MALTOMA of orbit: Fluorodeoxyglucose positron emission tomography/computed tomography images of a patient with extranodal marginal zone lymphoma of left orbit. Maximum intensity projection image (a) shows no systemic lymphomatous involvement. Although fluorodeoxyglucose avidity of MALTOMA is variable, often it shows moderate fluorodeoxyglucose uptake (b and c) which enables them to be detected in positron emission tomography

routine use of FDG-PET for staging. A literature review by Zanni *et al*. reported that the sensitivity of FDG-PET/CT for detecting primary lesion in low-grade OAL was 66% and for detecting systemic disease was 80%.[16] FDG-PET may also be helpful in radiotherapy planning. FDG avidity correlates with cellular proliferation; thus, dose escalation can be contemplated in lesion with high uptake.[17] Thus, FDG-PET/CT may be useful for radiation treatment planning, response evaluation, and follow-up of OAL.

Granulocytic Sarcoma

Granulocytic sarcomas (GSs) are rare extramedullary presentation of acute myeloid leukemia (AML) and occur in about 2%–8% of cases. Common sites of presentation include bones, lymph nodes, skin, breast, and rarely in gastrointestinal tract or genitourinary tract or in the head neck region. Orbital GS (OGS), although rare in adults, is relatively common in pediatric patients with AML. M2, M4, and M5 are the common subtype of AML associated with OGS. There is no consensus on optimal treatment of OGS and recently external beam radiotherapy is being tried in addition to the standard chemotherapy with cytosine arabinoside.[18] FDG-PET/CT has been evaluated as a noninvasive diagnostic tool for the identification of extramedullary disease in patients with AML [Figure 12]. Although FDG uptake of OGS is variable, it often shows moderate uptake to be detected in PET/CT. In a study done by Stölzel *et al*. in ten patients with GS, FDG uptake was present in all, but one patient and PET/CT detected additional extramedullary/multifocal disease in about 60% of patients. Multifocal disease is usually associated with adverse prognosis. Few studies have also demonstrated the potential clinical utility of PET/CT in monitoring response to treatment and in early identification of relapse of extramedullary disease during induction or at the end of chemotherapy.[19]

Orbital Metastases

Metastases to the orbit are estimated to account for approximately 20% of all orbital neoplasm.[1] Breast cancer is the most common solid tumor metastasizing to orbit in adults [Figure 13], followed by lung and prostate carcinoma, while in pediatric population, it is neuroblastoma [Figure 14]. Blurring of vision, diplopia, proptosis, and pain are the common clinical features, but paradoxically patients can also have enophthalmos due to desmoplasia and fibrosis associated with the tumors. Although most patients with orbital metastases present with known primary [Figure 15], in about 15%–30%, orbital swelling is the presenting complain, and in half of them, conventional imaging fails to demonstrate the primary tumor.[20] The site of primary tumor is an important prognostic factor influencing the OS. Since most common tumor metastasizing to orbit is routinely FDG avid, PET/CT is an ideal noninvasive modality to localize the primary tumor, estimating disease burden, and assess response to novel treatment.

Neural Tumors of Orbit

Glioma, meningioma, and peripheral nerve sheath tumors (PNSTs) of the orbit constitute about 10% of the orbital tumors and are associated with neurofibromatosis-1 syndrome.[1] Glioma and meningioma are intraconal tumors which appear as fusiform swelling of optic nerve in a CT/MR scan. Meningioma shows uniform enhancement in contrast-enhanced CT/MR while the central optic nerve appears unenhanced giving "tram-track" appearance

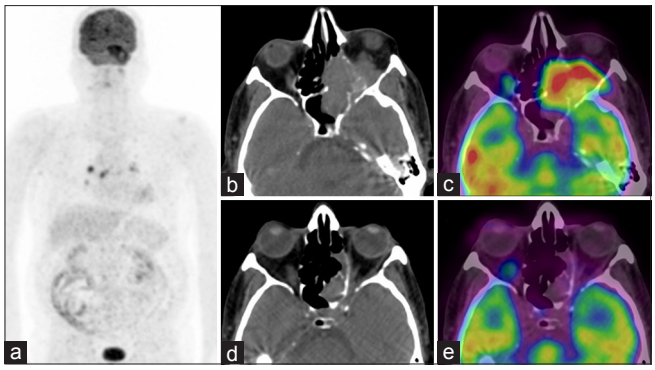

Figure 11: Diffuse large B-cell lymphoma of orbit: Fluorodeoxyglucose positron emission tomography/computed tomography images of a case of orbital diffuse large B-cell lymphoma. Maximum intensity projection image (a) shows no abnormal tracer distribution in rest of the body. (Note: uptake in thorax corresponds to calcified mediastinal nodes and not of lymphoma.) Axial images (b and c) show the hypermetabolic mass involving left orbit and adjacent left ethmoid sinus. A patient received radiotherapy and chemotherapy and positron emission tomography/computed tomography scan done at the end of treatment shows complete metabolic response (e) with residual nonviable tissue (d)

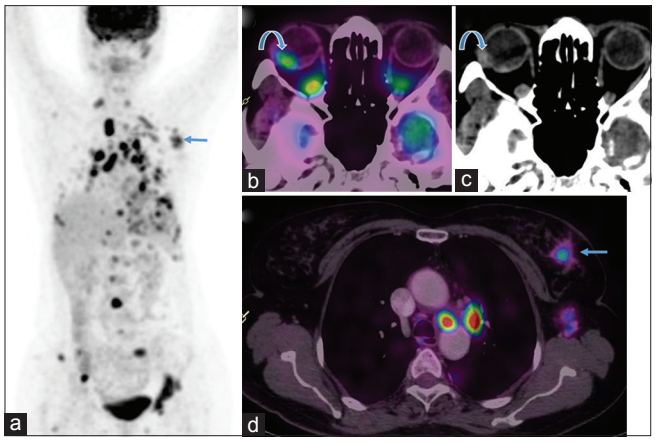

Figure 13: Choroidal metastases: A 67-year-old female presented with diminution of right eye vision. On examination was found to have left breast lump, biopsy of which revealed carcinoma. MIP image (a) of the PET scan shows tracer uptake in the breast mass (d) (arrow) and multiple distant metastases. Axial fusion (b) and computed tomography (c) images demonstrate right intraocular deposit (curved arrow). B-scan done later showed the deposit to be in choroid. Subsequently, the patient received radiotherapy to right eye and systemic chemotherapy

[Figure 16]. PNSTs (schwannoma and neurofibroma) of the orbit are generally extraconal tumors since they mostly arise from branches of ophthalmic nerve. Although these tumors are generally non-FDG avid, FDG-PET can be used to assess the grade of the glioma and PNST, especially in patients with neurofibromatosis. In addition to FDG-PET, molecular imaging targeting amino acid metabolism and somatostatin expression has shown promising results for the evaluation of glioma and meningioma, respectively.[21,22]

Conclusion

FDG-PET/CT is a highly sensitive diagnostic imaging tool for most orbital tumors as most of these demonstrate enhanced glucose metabolism. However, readers must be aware of the pitfalls of whole-body FDG-PET for assessing orbital tumors [Table 2]. FDG-PET with a dedicated contrast CT of the orbit (or in future PET/MRI) potentially can be a one stop imaging

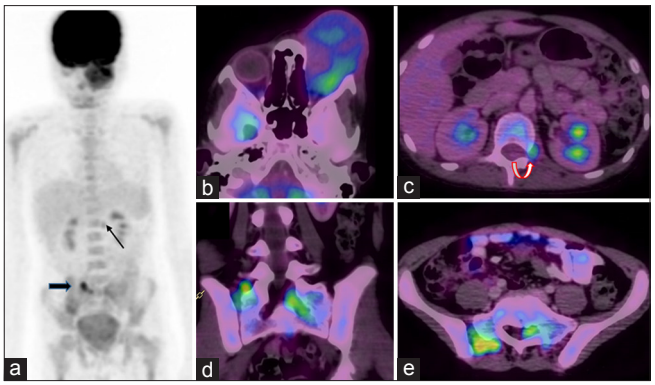

Figure 12: Orbital granulocytic sarcoma: A 11-year-old child with acute myeloid leukemia presented with orbital granulocytic sarcoma. Maximum intensity projection image (a) of the fluorodeoxyglucose positron emission tomography/computed tomography scan reveals focal increased tracer uptake in left orbital orbit, left paraspinal region (arrow) and multiple sites in pelvis (block arrow). Axial images reveal large soft-tissue mass in left orbit (b), lesion in L1–L2 junction (curved arrow) (c), left S1 canal (d), and mass near sacroiliac joint (e)

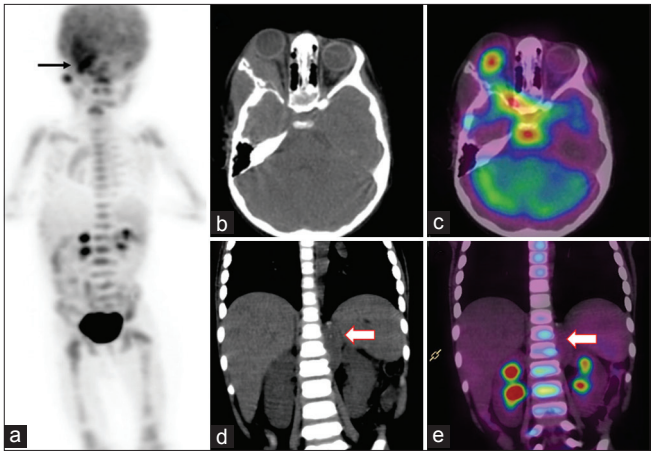

Figure 14: Orbital metastases from neuroblastoma: A 7-year-old male child presented with right orbital swelling and generalized weakness. Fine-needle aspiration cytology from orbital swelling reported malignant round cell tumor. Fluorodeoxyglucose positron emission tomography/computed tomography scan was done to evaluate disease burden. Maximum intensity projection image (a) shows uptake in right orbital region (arrow) and extensive uptake in skeletal system. Bone marrow biopsy confirmed the diagnosis of metastatic neuroblastoma. Axial images (b and c) reveal hypermetabolic orbital mass eroding bony orbit. Coronal (d and e) images show the primary tumor (block arrow) in left paraspinal region of abdomen

Table 2: Pitfalls of fluorodeoxyglucose-positron emission tomography/computed tomography in assessing orbital tumors

Variable FDG avidity of the orbital tumors
Intense physiological uptake in extraocular muscles
Partial volume effect due to small volume of tumor
Susceptibility for artifacts as orbit is in the edge of the field of view in the whole-body imaging

FDG: Fluorodeoxyglucose

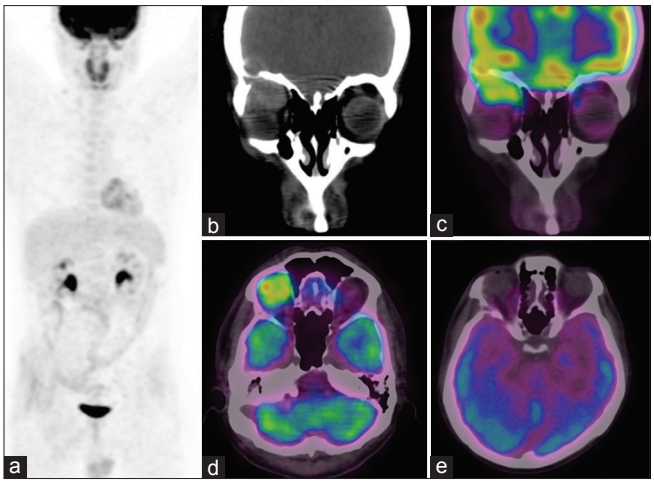

Figure 15: Orbital metastases from Ewing's sarcoma: Treated case of Ewing's sarcoma of iliac bone presented with right eye proptosis. Fine-needle aspiration cytology of the orbital mass was consistent with disease recurrence. Positron emission tomography/computed tomography was done to assess the metastases and plan appropriate treatment. Maximum intensity projection image (a) confirms no other site of metastases. Computed tomography (b) and the fusion images (c and d) show soft-tissue mass in superior aspect of the right orbit with erosion of roof of orbit. Subsequently, a patient received radiotherapy to right orbit and posttherapy scan image (e) revealed complete metabolic response

for characterization of primary malignancy, staging the cancer by assessing locoregional/distant spread of the disease, assessing response to treatment and earlier detection of disease recurrence.

Financial support and sponsorship

Nil.

Conflicts of interest

There are no conflicts of interest.

References

1. Shields JA, Shields CL, Scartozzi R. Survey of 1264 patients with orbital tumors and simulating lesions: The 2002 Montgomery lecture, part 1. Ophthalmology 2004;111:997-1008.
2. Chandra P, Purandare N, Shah S, Agrawal A, Rangarajan V. Common patterns of perineural spread in head-neck squamous cell carcinoma identified on fluoro-deoxyglucose positron emission tomography/computed tomography. Indian J Nucl Med 2016;31:274-9.
3. Freton A, Chin KJ, Raut R, Tena LB, Kivelä T, Finger PT, *et al.* Initial PET/CT staging for choroidal melanoma: AJCC correlation and second nonocular primaries in 333 patients. Eur J Ophthalmol 2012;22:236-43.
4. Finger PT, Kurli M, Reddy S, Tena LB, Pavlick AC. Whole body PET/CT for initial staging of choroidal melanoma. Br J Ophthalmol 2005;89:1270-4.
5. Kurli M, Chin K, Finger PT. Whole-body 18 FDG PET/CT imaging for lymph node and metastatic staging of conjunctival melanoma. Br J Ophthalmol 2008;92:479-82.
6. Wali UK, Al-Mujaini A. Sebaceous gland carcinoma of the eyelid. Oman J Ophthalmol 2010;3:117-21.
7. Shields JA, Demirci H, Marr BP, Eagle RC Jr., Shields CL. Sebaceous carcinoma of the eyelids: Personal experience with 60 cases. Ophthalmology 2004;111:2151-7.

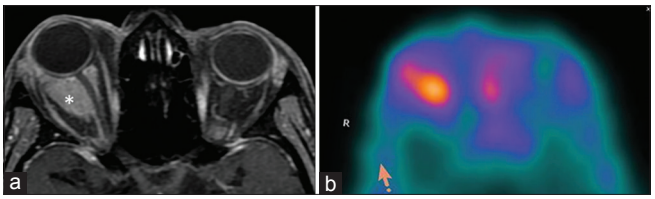

Figure 16: Optic nerve sheath meningioma: Appears as intraconal mass which enhances uniformly (asterisk) in contrast enhanced computed tomography/magnetic resonance image (a) with central nonenhancing optic nerve giving the appearance of "tram track." This finding differentiates meningioma from glioma; however, it can also be seen in pseudotumors and other tumors. Demonstration of somatostatin expression by molecular imaging (b) has high diagnostic accuracy for diagnosis of meningioma

8. Preechawai P, Della Roccad RC, Della Rocca D, Schaefer S, McCormack S. Transitional cell carcinoma of the lacrimal sac. J Med Assoc Thai 2005;88:138-42.
9. Tafti BA, Shaba W, Li Y, Yevdayev E, Berenji GR. Staging and follow-up of lacrimal gland carcinomas by 18F-FDG PET/CT imaging. Clin Nucl Med 2012;37:e249-52.
10. Jurdy L, Merks JH, Pieters BR, Mourits MP, Kloos RJ, Strackee SD, *et al.* Orbital rhabdomyosarcomas: A review. Saudi J Ophthalmol 2013;27:167-75.
11. Viswanathan S, George S, Ramadwar M, Shet T, Arora B, Laskar S, *et al.* Extraconal orbital tumors in children – A spectrum. Virchows Arch 2009;454:703-13.
12. Finger PT, Harbour JW, Karcioglu ZA. Risk factors for metastasis in retinoblastoma. Surv Ophthalmol 2002;47:1-6.
13. Radhakrishnan V, Kumar R, Malhotra A, Bakhshi S. Role of PET/CT in staging and evaluation of treatment response after 3 cycles of chemotherapy in locally advanced retinoblastoma: A prospective study. J Nucl Med 2012;53:191-8.
14. Freeman C, Berg JW, Cutler SJ. Occurrence and prognosis of extranodal lymphomas. Cancer 1972;29:252-60.
15. Demirci H, Shields CL, Karatza EC, Shields JA. Orbital lymphoproliferative tumors: Analysis of clinical features and systemic involvement in 160 cases. Ophthalmology 2008;115:1626-31, 1631.e1-3.
16. Zanni M, Moulin-Romsee G, Servois V, Validire P, Bénamor M, Plancher C, *et al.* Value of 18FDG PET scan in staging of ocular adnexal lymphomas: A large single-center experience. Hematology 2012;17:76-84.
17. Katayama E, Isao A, Kazuya I, Chikae K, Yoko M, Takayuki S, *et al*. FDG-PET may be useful in radiation therapy for indolent MALT lymphoma. Int J Radiat Oncol Biol Phys 2013;87:S555.
18. Ohanian M, Borthakur G, Quintas-Cardama A, Mathisen M, Cortés JE, Estrov Z, *et al.* Ocular granulocytic sarcoma: A case report and literature review of ocular extramedullary acute myeloid leukemia. Clin Lymphoma Myeloma Leuk 2013;13:93-6.
19. Stölzel F, Röllig C, Radke J, Mohr B, Platzbecker U, Bornhäuser M, *et al.* ^{18}F-FDG-PET/CT for detection of extramedullary acute myeloid leukemia. Haematologica 2011;96:1552-6.
20. Magliozzi P, Strianese D, Bonavolontà P, Ferrara M, Ruggiero P, Carandente R, *et al.* Orbital metastases in Italy. Int J Ophthalmol 2015;8:1018-23.
21. Moharir M, London K, Howman-Giles R, North K. Utility of positron emission tomography for tumour surveillance in children with neurofibromatosis type 1. Eur J Nucl Med Mol Imaging 2010;37:1309-17.
22. Valotassiou V, Leondi A, Angelidis G, Psimadas D, Georgoulias P. SPECT and PET imaging of meningiomas. Scientific World J 2012;2012:412580.